polymers

MDPI

Article

Preparation and Characterization of Chitosan/Soy Protein Isolate Nanocomposite Film Reinforced by Cu Nanoclusters

Kuang Li [1,2,3], Shicun Jin [1,2,3], Xiaorong Liu [1,2,3], Hui Chen [1,2,3,*], Jing He [1,2,3,*] and Jianzhang Li [1,2,3,*]

1 Key Laboratory of Wood Materials Science and Utilization, Beijing Forestry University, Ministry of Education, Beijing 100083, China; kuangli@bjfu.edu.cn (K.L.); jinsc1994@bjfu.edu.cn (S.J.); happyrong1993@bjfu.edu.cn (X.L.)
2 Beijing Key Laboratory of Wood Science and Engineering, Beijing Forestry University, Beijing 100083, China
3 College of Materials Science and Technology, Beijing Forestry University, Beijing 100083, China
* Correspondence: chenhui@bjfu.edu.cn (H.C.); hejing2008@sina.com (J.H.); lijzh@bjfu.edu.cn (J.L.); Tel.: +86-010-6233-6912 (H.C. & J.H. & J.L.)

Academic Editor: Alexander Böker
Received: 26 May 2017; Accepted: 23 June 2017; Published: 25 June 2017

Abstract: Soy protein isolate (SPI) based films have received considerable attention for use in packaging materials. However, SPI-based films exhibit relatively poor mechanical properties and water resistance ability. To tackle these challenges, chitosan (CS) and endogenous Cu nanoclusters (NCs) capped with protein were proposed and designed to modify SPI-based films. Attenuated total reflectance-Fourier transform infrared spectroscopy and X-ray diffraction patterns of composite films demonstrated that interactions, such as hydrogen bonds in the film forming process, promoted the cross-linking of composite films. The surface microstructure of CS/SPI films modified with Cu NCs was more uniform and transmission electron microscopy (TEM) showed that uniform and discrete clusters were formed. Compared with untreated SPI films, the tensile strength and elongation at break of composite films were simultaneously improved by 118.78% and 74.93%, respectively. Moreover, these composite films also exhibited higher water contact angle and degradation temperature than that of pure SPI film. The water vapor permeation of the modified film also decreased. These improved properties of functional bio-polymers show great potential as food packaging materials.

Keywords: soy protein isolate; Cu nanoclusters; chitosan; nanocomposite film; mechanical properties; water vapor barrier

1. Introduction

Polymer nanocomposites have emerged as an important research field in order to confer materials with superior properties [1,2]. Due to the advantages over conventional petroleum-based materials, researchers are committed to developing biopolymer-based films for use in packaging materials and coating industries [3,4]. Soy protein isolate (SPI) is a plant protein that is a reproducible resource, is safe, has good film-forming ability, and biocompatibility [5]. SPI-based films exhibit significant potential applications in the biosciences and biotechnology [6,7]. However, films obtained from unmodified SPI have some weaknesses in mechanical properties such as tensile strength and flexibility, which are critical issues for commercial applications [8]. Many traditional methods have been applied by previous studies, including different processing methods [9,10], blending organic or inorganic materials [11,12], and chemical cross-linking [13]. However, these efforts did not simultaneously improve the stiffness and flexibility of biopolymer films. González [14] reported that with the addition

of starch nanocrystals, the tensile strength (TS) of SPI films could increase from 1.10 to 5.08 MPa, but the elongation at break (EB) of SPI film would decrease from 65.95% to 21.35%. Alipoormazandarani [4] reported that films modified with halloysite nanoclay showed enhanced TS, but poor EB. The reports of Jensen and Zhang also demonstrated that cellulose fibers or TiO_2 improved the strength of films with a loss of flexibility [15,16]. Therefore, it is necessary to enhance both the strength and flexibility of SPI-based films simultaneously for further application.

As one of the most abundant natural biopolymers, chitosan is the *N*-deacetylated derivative of chitin and contains β-1-4 linked 2-amino-2-deoxy-D-glucopyranose repeat units [17,18]. Previous studies have shown that chitosan may interact with proteins to form films with enhanced mechanical properties [19–21]. However, natural defects and compatibility problems of the components might limit further application of these CS/SPI composite films. Meanwhile, functional nanomaterials have attracted much attention in recent decades as these nanoparticles could offer promising alternatives for improving polymer properties and extending their application fields [22,23]. Cu nanoclusters (NCs), composed of a few to hundreds of atoms, are defined as particles less than 2 nm and are considered to be novel potential nanomaterials [24,25]. The dimension of this nanoparticle approaches the Fermi wavelength of electrons. The discrete energy levels of electrons make the chemical, electronic and optical properties of this nanoparticle significantly different from conventional bulk materials [26,27]. In particular, Cu NCs exhibit good biocompatibility and multifunctional surface chemistry; thus, this nanomaterial may produce great results in improving the strength and compatibility of polymers [28].

Therefore, the objective of this work was to investigate the effects of chitosan and Cu NCs on the mechanical properties of SPI-based films. The modified SPI-based nanocomposite films were investigated by attenuated total reflectance-Fourier transform infrared (ATR FT-IR) spectroscopy, X-ray diffraction (XRD), contact angles determination, scanning electron microscopy (SEM), thermogravimetric analysis (TGA), moisture content (MC), and water vapor permeability (WVP). These characterizations indicated that CS and Cu NCs had a large influence on the structure, surface hydrophobicity, morphology, thermal stability, moisture content and water vapor permeability of SPI-based films, which are important properties of composite films in packaging material applications.

2. Materials and Methods

2.1. Materials

SPI with 2.0% moisture and 95% protein content was purchased by Yuwang Ecological Food Industry Co., Ltd. (Shandong, China). Copper sulfate anhydrous was obtained from Beijing Chemical Works (Beijing, China). Chitosan (95% deacetylation, biochemical reagent grade) was provided by Sinopharm Chemical Reagent Co., Ltd. (Beijing, China). Sodium hydroxide (analytical grade) was provided from Beijing Chemical Reagents (Beijing, China). Deionized water was used to prepare all aqueous solutions.

2.2. Preparation of SPI–Cu NCs

An amount of 4.0 g SPI was dissolved in 80 g distilled water with constant magnetic stirring (RW20 digital, IKA, Staufen, Germany) at 200 rpm to prepare the SPI solutions. Next, 8 mL $CuSO_4$ solution (20 mmol/L) was added into these SPI solutions. The mixed solutions were stirred at 200 rpm at 25 °C for 10 min and adjusted pH to 12 with the NaOH solution. The mixture was heated under constant stirring at 75 °C for 8 h to prepare the SPI–Cu NCs solutions.

2.3. Preparation of CS/SPI–Cu NCs Composite Films

Chitosan solution (1%, *w*/*w*) was prepared by dissolving chitosan in acetic acid solution (2%, *v*/*v*) with continuous stirring at 200 rpm. Then, 8.0 g chitosan solution and 2.0 g glycerol was added into 80 g SPI–Cu NCs solution that was prepared before. According to the report of Jia et al. [29], chitosan was only soluble in acidic solution and the film prepared at pH 3.0 displayed better water barrier

and mechanical properties. Therefore, the pH of the mixing solution was adjusted to 3.0. Next, the mixtures were stirred constantly at 200 rpm at 85 °C for 30 min and then poured into Teflon-coated plates. The films were vacuum-dried at 45 °C for 24 h. According to Schmid, M., et al. [30], all the films were tested at the same time, about a week after production, and the results were reproducible.

2.4. Characterization of SPI/CS Nanocomposite Films

2.4.1. Transmission Electron Microscopy (TEM)

SPI–Cu NCs solutions were analyzed by TEM. SPI–Cu NCs solutions were poured on a copper wire mesh and dried in an oven at 45 °C for 30 min. Next, TEM images were observed on a JEM-1010 transmission electron microscopy (JEOL, Tokyo, Japan).

2.4.2. Attenuated Total Reflectance-Fourier Transform Infrared Spectroscopy

Attenuated total reflectance-Fourier transform infrared (ATR-FTIR) spectra were performed by a Nicolet 6700 spectrometer (Thermo Scientific, Madison, WI, USA) with a range of 4000–650 cm^{-1} and 32 scans.

2.4.3. X-Ray Diffraction Analysis

X-ray diffraction (XRD) was used by a D8 advance diffractometer (Bruker, Karlsruhe, Germany) with a radiation source of Cu–Ka. The data were measured from 5° to 60° with a 0.02° step interval at a voltage of 45 kV.

2.4.4. Scanning Electron Microscope

Scanning electron microscopy (SU8010, Hitachi, Tokyo, Japan) was carried out to analyze the surface morphologies of composite films with an acceleration voltage of 5 kV.

2.4.5. Mechanical Properties

Mechanical properties of the nanocomposite films were measured with a tensile testing machine (INSTRON 3365, INSTRON, Norwood, MA, USA) at a speed of 20 mm/min at 25 °C and a relative humidity of 50% as per the report of Li et al. [31]. Each film sample was cut into pieces with a size of 10 mm × 80 mm. Five specimens were measured to obtain the average values of tensile strength (TS), Young's modulus (E) and elongation at break (EB).

2.4.6. Surface Contact Angles

Surface hydrophobicity was characterized by water contact angle (OCA20, DataPhysics Instruments GmbH, Filderstadt, Germany). Prior to testing, all samples were conditioned in a saturated K_2CO_3-regulated desiccator at 50% ± 2% relative humidity and 25 °C. A drop of distilled water (3 μL) was dropped onto the surface of film samples (20 mm × 80 mm). Five replicates were tested for each film.

2.4.7. Thermo-Gravimetric Analysis

The thermal stability of films was characterized by a Q50 TGA analyzer (TA Instrument, New Castle, DE, USA). Films were dried at 105 °C for 24 h and then heated from 10 °C to 600 °C at a rate of 10 °C/min in a nitrogen atmosphere (100 mL/min).

2.4.8. Moisture Content

Five specimens were tested to calculate the moisture content of each film, and all films were conditioned in a saturated K_2CO_3-regulated (50% ± 2% relative humidity) desiccator at 25 °C before testing. Film specimens were weighted and recorded as m_0, and then dried in an air-circulating oven at 105 °C for 24 h and weighed (m_d). Moisture content for each film was calculated as follows:

$$\text{MC}\ (\%) = (m_0 - m_d)/m_0 \times 100 \quad (1)$$

2.4.9. Water Vapor Permeability

Water vapor permeability was tested by a water vapor permeability tester (TSY-T1, Labthink Instrument, Jinan, China) as per the ASTM E96-01 standard method. Distilled water was poured into the test dish and placed in the controlled chamber at 25 °C and 50% relative humidity for 11 h. Five samples were tested for each film. The WVP was calculated as follows:

$$\text{WVP} = \text{WVTR}x/[P_0(\text{RH}_1 - \text{RH}_2)] \quad (2)$$

where WVTR is the measured water vapor transmission rate (g/m^2 h) through each film, x is related to the thickness (mm) of the film; P_0 is related to the vapor pressure of pure water (25 °C, 3.169 kPa); and ($RH_1 - RH_2$) is the relative humidity gradient used in the experiment which was controlled at 50% during the test.

2.4.10. Statistical Analysis

Experiments were done in five replicates and data were analyzed by the analysis of variance (ANOVA) with the SPSS computer program. Tukey's test was conducted to determine the post hoc multiple comparisons with the level of significance set at $p < 0.05$.

3. Results

3.1. Characterization of SPI–Cu NCs

The morphology and size of Cu NCs synthesized in the SPI substrate were characterized by transmission electron microscopy (TEM) images. As shown in Figure 1, Cu NCs were prepared by using an SPI template, which showed uniform and discrete clusters in the prepared solution. The average diameter of Cu NCs was approximately 50 nm (Figure 1b).

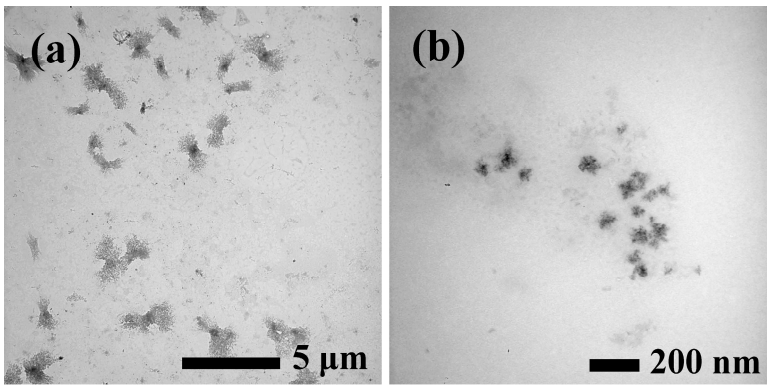

Figure 1. Transmission electron microscopy (TEM) images of soy protein isolate (SPI) based Cu nanoclusters (NCs) in solution (**a**) and (**b**).

3.2. Structural Analysis

Attenuated total reflectance-Fourier transform infrared (ATR-FTIR) spectra were performed to investigate the changes of the functional groups in SPI-based film. As seen in Figure 2a, all SPI-based films exhibited similar spectra. The peaks at 1626, 1532 and 1231 cm^{-1} were assigned to amide I (C–O stretching), amide II (N–H bending) and amide III (C–H and N–H stretching), respectively [10]. Amide I and II of the SPI films treated by Cu NCs shifted to higher wavenumbers, which suggested the possible existence of hydrogen bonding between these polymers [32]. The peak at 2928 cm^{-1} appeared due to C–H stretching [2]. The broad absorption band observed around 3274 cm^{-1} was

attributable to free and bound O–H and N–H groups, which formed hydrogen bonding with the carbonyl group of the peptide linkage in the protein matrix [5]. The increase in vibrational wavenumber of O–H and N–H vibration bands could be indicative of interactions between SPI and Cu NCs in composite film via hydrogen bonding [33]. These changes confirmed that the structures of SPI and chitosan were more unfolded and loose, which might make the films expose more polar and functional groups [34]. These interactions determined the mechanical properties and hydrophobicity of composite films, which were attributed to the effects of hydrogen bonds or electrostatic interactions between chitosan and Cu NCs.

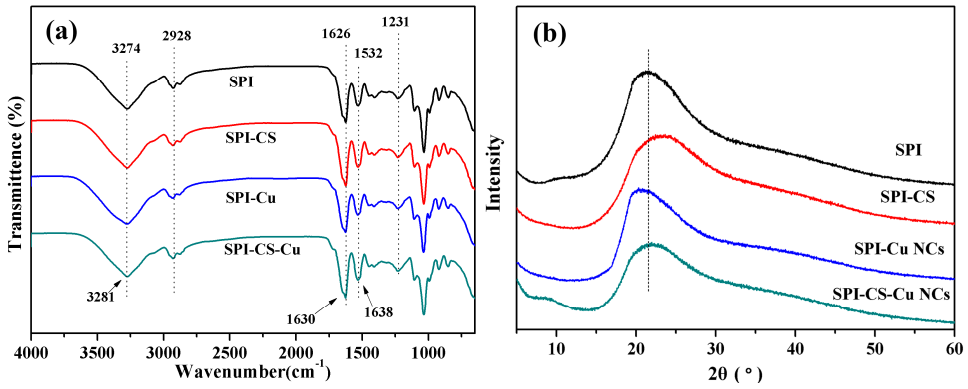

Figure 2. (**a**) Attenuated total reflectance-Fourier transform infrared (ATR-FTIR) spectra; and (**b**) X-ray diffraction (XRD) patterns of soy protein isolate (SPI) based films unmodified and modified with chitosan (CS) and Cu nanoclusters (NCs).

X-ray diffraction (XRD) was conducted to investigate the changes of the structure of SPI-based films prepared with chitosan and Cu NCs. Figure 2b displays the XRD data of the SPI-based films untreated and treated with chitosan and Cu NCs. The XRD patterns of the SPI-based films were similar, and all films exhibited a relatively strong characteristic peak at $2\theta = 22^{\circ}$, which represented the β-sheet structures of the SPI secondary structure [35]. The intensity of the peaks at $2\theta = 22^{\circ}$ of the modified films were slightly lower than that of the control film, due to the destruction of the SPI structure during the formation of nanocomposite films, indicating that Cu NCs changed the conformation of SPI and decreased the regular arrangement of the molecular chains. These results might make composite expose more active groups and prompt further reactions [36].

3.3. Micromorphology of SPI-Based Film

SEM analysis was performed to investigate the microstructure of the composite films and the compatibility of the polymers. As seen in Figure 3a, the control film exhibited a smooth, compact and continuous surface, indicating that SPI had good film-forming ability. However, the images (Figure 3b) of SPI-based films modified with chitosan showed a relatively rougher surface morphology; there were some agglomerates on the surface of SPI–CS film, suggesting the formation of a heterogeneous structure. This phenomenon indicated the presence of thermodynamic incompatibility and phase segregation of SPI and chitosan [37]. The SPI–Cu NCs films showed a relatively coarse surface (Figure 3c), which may have been caused by the dispersion of Cu NCs. In particular, the surface of the CS/SPI film was more homogeneous (Figure 3d) with the incorporation of Cu NCs, and the agglomerates became more regular and uniform than those of the SPI–CS film. This change demonstrated that uniform dispersion of Cu NCs in the film matrix and Cu NCs may improve the phase compatibility of the blend components. SEM observations suggested that chitosan and Cu NCs had an important role in the organization of composite, which in turn determined the properties of SPI-based films. The compatibility of these polymers was more likely to enhance the molecular interactions in the SPI matrix, such as hydrogen bonding and electrostatic interactions, resulting in the improved mechanical and physical properties of the composited films.

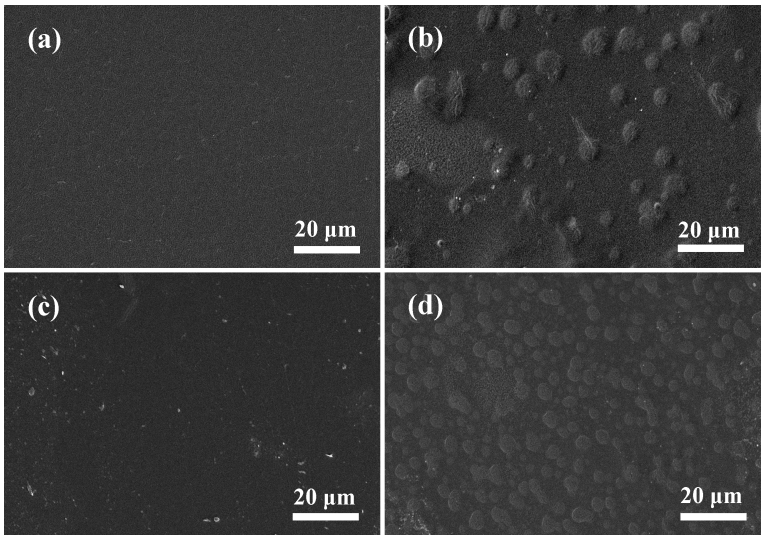

Figure 3. Scanning electron microscope (SEM) images of the surface of soy protein isolate (SPI) based films unmodified and modified with chitosan (CS) and Cu nanoclusters (NCs): (**a**) SPI; (**b**) SPI–CS; (**c**) SPI–Cu NCs; and (**d**) SPI–CS–Cu NCs.

3.4. Physical and Mechanical Properties

Mechanical properties of composite films are very important and determine the potential application of films as packaging materials. Tensile strength (TS), Young's modulus (*E*), and elongation at break (EB) of SPI-based films were analyzed and are shown in Table 1.

Table 1. Tensile strength (TS), Young's modulus (*E*) and elongation at break (EB) of soy protein isolate (SPI) based films unmodified and modified with chitosan (CS) and Cu nanoclusters (NCs).

Samples	Thickness	TS	*E*	EB
	(mm)	(MPa)	(MPa)	(%)
SPI	0.213 (0.019) ^{b}	2.29 (0.16) ^{c}	58.75 (2.52) ^{c}	17.63 (0.09) ^{c}
SPI–CS	0.190 (0.024) ^{c}	3.02 (0.28) ^{b}	67.89 (3.29) ^{c}	62.86 (0.04) ^{a}
SPI–Cu NCs	0.234 (0.015) ^{a}	3.55 (0.21) ^{b}	149.20 (3.40) ^{b}	17.05 (0.17) ^{c}
SPI–CS–Cu NCs	0.240 (0.026) ^{a}	5.01 (0.34) ^{a}	197.50 (4.05) ^{a}	30.84 (0.13) ^{b}

The values in parenthesis are the standard deviation, $^{a–c}$ Two means in the same column followed by the same letter are not significantly ($p > 0.05$) different through the Tukey's multiple range test.

Without a plasticizer, SPI-based film exhibited low strength and flexibility due to the rigid and brittle properties of protein. However, with the modification of chitosan, the TS values of SPI–CS films increased slightly, indicating that the addition of chitosan could improve the strength of SPI films slightly, which was attributed to the hydrogen bonding in the polymers [21]. Moreover, the results also showed that the EB values of composite films obviously increased from 17.63% to 62.86% with the modification of chitosan, indicating that chitosan might cause a plasticizing effect on the protein matrix [38]. Meanwhile, it was reported that intermolecular interactions were most likely established in these polymers, such as ionic and hydrophobic interactions [39]. Therefore, the flexibility of composite films was obviously improved.

Moreover, the TS and E values of SPI-based films modified with chitosan and Cu NCs showed an obvious increase with values of 5.01 MPa and 197.50 MPa, respectively. The significant enhancement of mechanical strength could be attributed to the effect of Cu NCs on the protein matrix and interfacial compatibility [40]; this result was supported by previous SEM analysis. Therefore, the structure of the composite film exhibited increased contact areas that promoted interactions in polymers, which

resulted in a higher degree of molecular cross-linking and physically entangled structure in SPI–CS films. It is worth noting that compared with untreated SPI film, the TS and E values of SPI-based films modified with chitosan and Cu NCs were simultaneously increased, suggesting that the modification of chitosan and Cu NCs had a great effect on the reinforcement of the SPI-based films.

3.5. Contact Angles Analysis

The surface hydrophobicity was evaluated by measuring the contact angle of a water droplet on the surface of composite films. Generally, protein films possess high-water sensitivity, which is not desirable for packaging applications. Compared with the control film, the water contact angle of SPI–CS films increased, which could be attributed to the relatively high hydrophobic property of chitosan (Figure 4). Compared with the SPI film, the SPI–Cu NCs film exhibited a lower water contact angle, indicating a highly hydrophilic and wettable surface. This feature was due to the high content of polar groups on the surface of composite films [41]. These observations suggested that chitosan might result in the exposure of hydrophobic groups of soy proteins, thus increasing the surface hydrophobicity of films [29]. Therefore, the results demonstrated that SPI-based films modified with chitosan and Cu NCs exhibited preferable surface hydrophobicity and had great potential to overcome the limitation of hygroscopic property.

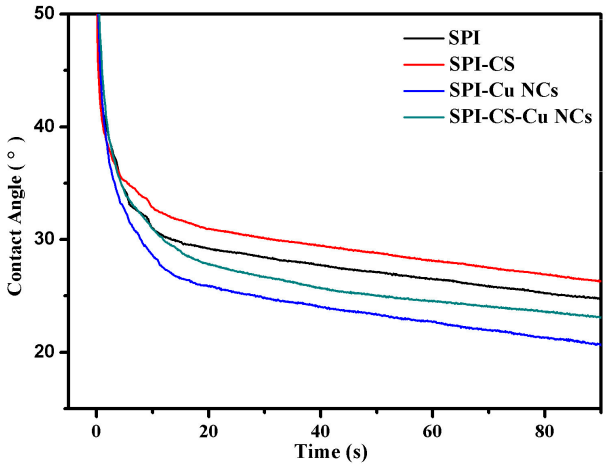

Figure 4. Water contact angles of soy protein isolate (SPI) based films unmodified and modified with chitosan (CS) and Cu nanoclusters (NCs).

3.6. Thermo-Gravimetric Analysis

The thermal stability of SPI-based films was investigated using thermo gravimetric (TG) and derivative thermo gravimetric (DTG), as shown in Figure 5. There were four steps to achieve the thermal degradation of composite films in the temperature range of 100–600 °C. The first step was from room temperature to 120 °C and corresponded to the loss of water in films. The second step of 120 °C to 280 °C was due to the degradation of glycerol. The degradation rate of films appeared between 280 °C and 450 °C, and was attributed to the decomposition of the SPI matrix. The last step was from 450 °C to 600 °C for the carbonized polymers in films [42].

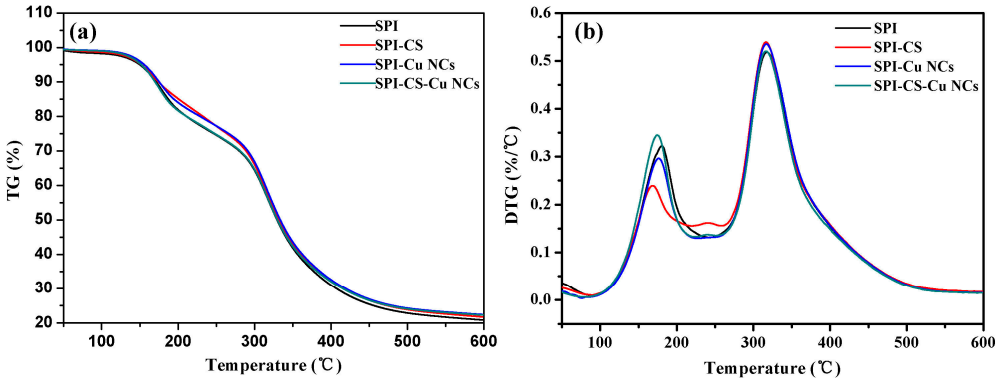

Figure 5. (**a**) Thermo gravimetric (TG) and (**b**) derivative thermo gravimetric (DTG) curves of soy protein isolate (SPI) based films unmodified and modified with chitosan (CS) and Cu nanoclusters (NCs).

These results suggested that the SPI–Cu films modified with chitosan showed a higher heat resistance and degradation temperature than the control film. It was reported that chitosan had a main weight loss at 300 °C, which might explain why the composite films exhibited lower rates of decomposition below 300 °C. Therefore, the modification of chitosan and Cu NCs might improve the thermal stability of SPI-based films.

3.7. Water Resistance

Moisture content (MC) was related to the water resistance ability of films. Table 2 shows the moisture content for the control film and the SPI-based films with chitosan and Cu NCs. Compared with the control film, the SPI based films modified with chitosan (CS) and Cu nanoclusters (NCs) presented an obvious increase in the value of MC, which was due to the structural changes of the films made by the swelling of the hydrophilic fraction of the polymer matrix [29].

Table 2. Moisture content (MC) and water vapor permeation (WVP) of soy protein isolate (SPI) based films unmodified and modified with chitosan (CS) and Cu nanoclusters (NCs).

Samples	Moisture content (%)	Water vapor permeation ($g \cdot mm \cdot h^{-1} \cdot m^{-2} \cdot kPa^{-1}$)
SPI	9.89 (1.3) ^{c}	1.16 (0.15) ^{b}
SPI–CS	15.40 (1.6) ^{a}	1.27 (0.19) ^{a}
SPI–Cu NCs	11.84 (1.1) ^{b}	0.99 (0.12) ^{c}
SPI–CS–Cu NCs	14.09 (1.8) ^{a}	1.10 (0.16) ^{b}

The values in parenthesis are the standard deviations, $^{a–c}$ Two means in the same column followed by the same letter are not significantly ($p > 0.05$) different through the Tukey's multiple range test.

Meanwhile, water vapor barrier properties were also investigated by water vapor permeation (WVP). The resistance of the films against water vapor was highly associated with the micro-paths in the network microstructures of the SPI matrix. Without modification, the water vapor permeability of the SPI-based films was poor due to the hydrophilicity of the protein molecule. As shown in Table 2, the WVP of the SPI–CS film was higher than that of the control film. This change might have resulted from the phase separation between the SPI and chitosan during preparation, and the addition of chitosan to the SPI solution might decrease the intermolecular interactions (such as hydrogen binding) and increase the electrostatic repulsion between these two polymers [39]. Compared with the SPI and SPI–CS films, the WVP of SPI-based films modified with Cu NCs was significantly decreased, indicating a better water vapor barrier property of the composite films. The lower WVP of the composite films modified with Cu NCs could be due to the improved cross-linking of the SPI chains

as well as the strong interactions between polymers [43,44]. With the modification of Cu NCs, the compatibility of SPI and chitosan molecules might be improved, which resulted in increased circuitous routes of films [17].

4. Conclusions

In summary, we synthesized water-dispersed Cu NCs capped with the soy protein isolate with a facile method, and used Cu NCs and chitosan to modify the mechanical properties of SPI-based films. Compared with unmodified films, the modification of chitosan and Cu NCs improved the strength and flexibility of the composite films where the TS and EB values of the SPI–CS–Cu NCs films increased by 118.78% and 74.93%, respectively, which might have been caused by the interactions in the SPI matrix. Compared with the TS of soybean protein film [11], the TS of SPI–CS–Cu NCs films significantly increased from 3.54 to 5.01 MPa, suggesting the reinforced mechanical property. The addition of Cu NCs improved the compatibility between the SPI and chitosan, thus the microstructures of the SPI-based films were more uniform. Meanwhile, with the modification of chitosan and Cu NCs, SPI-based films also showed a higher water contact angle and degradation temperature, suggesting better hydrophobicity and thermal stability of the composite films. Compared with isolated soy protein film [45], SPI–CS–Cu NCs film also led to a decrease in WVP, indicating superior water vapor barrier ability. The improved functional properties of this novel nanocomposite film contributed to its potential application in food packaging materials.

Acknowledgments: The authors are grateful for financial support from the Fundamental Research Funds for the Central Universities (BLX201601), the Beijing Natural Science Foundation (2151003) and the Special Fund for Forestry Research in the Public Interest (Project 201404501).

Author Contributions: Kuang Li and Hui Chen conceived the project and designed the experiments; Kuang Li, Shicun Jin and Xiaorong Liu performed the experiments and analysed the data; Kuang Li wrote the main manuscript text; Hui Chen, Jing He and Jianzhang Li supervised and directed the project; All authors reviewed the manuscript.

Conflicts of Interest: The authors declare no conflict of interest.

References

1. Müller, K.; Jesdinszki, M.; Schmid, M. Modification of functional properties of whey protein isolate nanocomposite films and coatings with nanoclays. *J. Nanomater.* **2017**, *2017*, 1–10. [CrossRef]
2. Weizman, O.; Dotan, A.; Nir, Y.; Ophir, A. Modified whey protein coatings for improved gas barrier properties of biodegradable films. *Polym. Adv. Technol.* **2017**, *28*, 261–270. [CrossRef]
3. Coltelli, M.-B.; Wild, F.; Bugnicourt, E.; Cinelli, P.; Lindner, M.; Schmid, M.; Weckel, V.; Müller, K.; Rodriguez, P.; Staebler, A.; et al. State of the art in the development and properties of protein-based films and coatings and their applicability to cellulose based products: An extensive review. *Coatings* **2016**, *6*, 1. [CrossRef]
4. Hammann, F.; Schmid, M. Determination and quantification of molecular interactions in protein films: A review. *Materials* **2014**, *7*, 7975–7996. [CrossRef]
5. Zink, J.; Wyrobnik, T.; Prinz, T.; Schmid, M. Physical, chemical and biochemical modifications of protein-based films and coatings: An extensive review. *Int. J. Mol. Sci.* **2016**, *17*, 1376. [CrossRef] [PubMed]
6. Garrido, T.; Etxabide, A.; Peñalba, M.; de la Caba, K.; Guerrero, P. Preparation and characterization of soy protein thin films: Processing–properties correlation. *Mater. Lett.* **2013**, *105*, 110–112. [CrossRef]
7. Dash, S.; Swain, S.K. Effect of nanoboron nitride on the physical and chemical properties of soy protein. *Compos. Sci. Technol.* **2013**, *84*, 39–43. [CrossRef]
8. Morales, R.; Martinez, K.D.; Pizones Ruiz-Henestrosa, V.M.; Pilosof, A.M. Modification of foaming properties of soy protein isolate by high ultrasound intensity: Particle size effect. *Ultrason. Sonochem.* **2015**, *26*, 48–55. [CrossRef] [PubMed]
9. Kumar, R.; Anandjiwala, R.D.; Kumar, A. Thermal and mechanical properties of mandelic acid-incorporated soy protein films. *J. Therm. Anal. Calorim.* **2015**, *123*, 1273–1279. [CrossRef]

10. Belyamani, I.; Prochazka, F.; Assezat, G. Production and characterization of sodium caseinate edible films made by blown-film extrusion. *J. Food Eng.* **2014**, *121*, 39–47. [CrossRef]
11. Ciannamea, E.M.; Stefani, P.M.; Ruseckaite, R.A. Physical and mechanical properties of compression molded and solution casting soybean protein concentrate based films. *Food Hydrocoll.* **2014**, *38*, 193–204. [CrossRef]
12. Nur Hanani, Z.A.; Roos, Y.H.; Kerry, J.P. Use and application of gelatin as potential biodegradable packaging materials for food products. *J. Biol. Macromol.* **2014**, *71*, 94–102. [CrossRef] [PubMed]
13. Pan, H.; Jiang, B.; Chen, J.; Jin, Z. Blend-modification of soy protein/lauric acid edible films using polysaccharides. *Food Chem.* **2014**, *151*, 1–6. [CrossRef] [PubMed]
14. González, A.; Strumia, M.C.; Alvarez Igarzabal, C.I. Cross-linked soy protein as material for biodegradable films: Synthesis, characterization and biodegradation. *J. Food Eng.* **2011**, *106*, 331–338. [CrossRef]
15. González, A.; Alvarez Igarzabal, C.I. Nanocrystal-reinforced soy protein films and their application as active packaging. *Food Hydrocoll.* **2015**, *43*, 777–784. [CrossRef]
16. Jensen, A.; Lim, L.T.; Barbut, S.; Marcone, M. Development and characterization of soy protein films incorporated with cellulose fibers using a hot surface casting technique. *LWT Food Sci. Technol.* **2015**, *60*, 162–170. [CrossRef]
17. Zhang, W.; Chen, J.; Chen, Y.; Xia, W.; Xiong, Y.L.; Wang, H. Enhanced physicochemical properties of chitosan/whey protein isolate composite film by sodium laurate-modified TiO_2 nanoparticles. *Carbohydr. Polym.* **2016**, *138*, 59–65. [CrossRef] [PubMed]
18. Qin, Y.; Lu, X.; Sun, N.; Rogers, R.D. Dissolution or extraction of crustacean shells using ionic liquids to obtain high molecular weight purified chitin and direct production of chitin films and fibers. *Green Chem.* **2010**, *12*, 968. [CrossRef]
19. Wang, X.; Hu, L.; Li, C.; Gan, L.; He, M.; He, X.; Tian, W.; Li, M.; Xu, L.; Li, Y.; et al. Improvement in physical and biological properties of chitosan/soy protein films by surface grafted heparin. *J. Biol. Macromol.* **2016**, *83*, 19–29. [CrossRef] [PubMed]
20. Abugoch, L.E.; Tapia, C.; Villamán, M.C.; Yazdani-Pedram, M.; Díaz-Dosque, M. Characterization of quinoa protein-chitosan blend edible films. *Food Hydrocoll.* **2011**, *25*, 879–886. [CrossRef]
21. Boy, R.; Maness, C.; Kotek, R. Properties of chitosan/soy protein blended films with added plasticizing agent as a function of solvent type at acidic pH. *Int. J. Polym. Mater. Polym. Biomater.* **2015**, *65*, 11–17. [CrossRef]
22. Bugnicourt, E.; Kehoe, T.; Latorre, M.; Serrano, C.; Philippe, S.; Schmid, M. Recent prospects in the inline monitoring of nanocomposites and nanocoatings by optical technologies. *Nanomaterials* **2016**, *6*, 150. [CrossRef] [PubMed]
23. Muller, K.; Bugnicourt, E.; Latorre, M.; Jorda, M.; Echegoyen Sanz, Y.; Lagaron, J.M.; Miesbauer, O.; Bianchin, A.; Hankin, S.; Bolz, U.; et al. Review on the processing and properties of polymer nanocomposites and nanocoatings and their applications in the packaging, automotive and solar energy fields. *Nanomaterials* **2017**, *7*, 74. [CrossRef] [PubMed]
24. Tao, Y.; Li, M.; Ren, J.; Qu, X. Metal nanoclusters: Novel probes for diagnostic and therapeutic applications. *Chem. Soc. Rev.* **2015**, *44*, 8636–8663. [CrossRef] [PubMed]
25. Gao, W.; Wang, X.; Xu, W.; Xu, S. Luminescent composite polymer fibers: In situ synthesis of silver nanoclusters in electrospun polymer fibers and application. *Mater. Sci. Eng. C* **2014**, *42*, 333–340. [CrossRef] [PubMed]
26. Shang, L.; Nienhaus, G.U. Metal nanoclusters: Protein corona formation and implications for biological applications. *Int. J. Biochem. Cell Biol.* **2016**, *75*, 175–179. [CrossRef] [PubMed]
27. Shang, L.; Dong, S.; Nienhaus, G.U. Ultra-small fluorescent metal nanoclusters: Synthesis and biological applications. *Nano Today* **2011**, *6*, 401–418. [CrossRef]
28. Xu, H.; Suslick, K.S. Water-soluble fluorescent silver nanoclusters. *Adv. Mater.* **2010**, *22*, 1078–1082. [CrossRef] [PubMed]
29. Jia, D.; Fang, Y.; Yao, K. Water vapor barrier and mechanical properties of konjac glucomannan–chitosan–soy protein isolate edible films. *Food Bioprod. Process.* **2009**, *87*, 7–10. [CrossRef]
30. Schmid, M.; Reichert, K.; Hammann, F.; Stäbler, A. Storage time-dependent alteration of molecular interaction–property relationships of whey protein isolate-based films and coatings. *J. Mater. Sci.* **2015**, *50*, 4396–4404. [CrossRef]
31. Li, Y.; Chen, H.; Dong, Y.; Li, K.; Li, L.; Li, J. Carbon nanoparticles/soy protein isolate bio-films with excellent mechanical and water barrier properties. *Ind. Crops Prod.* **2016**, *82*, 133–140. [CrossRef]

32. Salavati-Niasari, M.; Davar, F.; Mazaheri, M. Synthesis and characterization of ZnS nanoclusters via hydrothermal processing from [bis (salicylidene) zinc (II)]. *J. Alloys Compd.* **2009**, *470*, 502–506. [CrossRef]
33. Li, K.; Chen, H.; Li, Y.; Li, J.; He, J. Endogenous Cu and Zn nanocluster-regulated soy protein isolate films: Excellent hydrophobicity and flexibility. *RSC Adv.* **2015**, *5*, 66543–66548. [CrossRef]
34. Arfat, Y.A.; Benjakul, S.; Prodpran, T.; Osako, K. Development and characterisation of blend films based on fish protein isolate and fish skin gelatin. *Food Hydrocoll.* **2014**, *39*, 58–67. [CrossRef]
35. Guerrero, P.; Stefani, P.M.; Ruseckaite, R.A.; de la Caba, K. Functional properties of films based on soy protein isolate and gelatin processed by compression molding. *J. Food Eng.* **2011**, *105*, 65–72. [CrossRef]
36. Guerrero, P.; Leceta, I.; Peñalba, M.; de la Caba, K. Optical and mechanical properties of thin films based on proteins. *Mater. Lett.* **2014**, *124*, 286–288. [CrossRef]
37. Ferreira, C.O.; Nunes, C.A.; Delgadillo, I.; Lopes-da-Silva, J.A. Characterization of chitosan-whey protein films at acid pH. *Food Res. Int.* **2009**, *42*, 807–813. [CrossRef]
38. Galus, S.; Kadzińska, J. Whey protein edible films modified with almond and walnut oils. *Food Hydrocoll.* **2016**, *52*, 78–86. [CrossRef]
39. Chen, H.; Lin, L.; Li, H.; Li, J.; Lin, J.-M. Aggregation-induced structuretransition of protein-stabilized zinc/copper nanoclusters for amplified chemiluminescence. *ACS Nano* **2015**, *9*, 2173–2183. [CrossRef] [PubMed]
40. Li, K.; Jin, S.; Chen, H.; He, J.; Li, J. A high-performance soy protein isolate-based nanocomposite film modified with microcrystalline cellulose and Cu and Zn nanoclusters. *Polymers* **2017**, *9*, 167–178. [CrossRef]
41. Tian, H.; Wang, Y.; Zhang, L.; Quan, C.; Zhang, X. Improved flexibility and water resistance of soy protein thermoplastics containing waterborne polyurethane. *Ind. Crops Prod.* **2010**, *32*, 13–20. [CrossRef]
42. Schmidt, V.; Giacomelli, C.; Soldi, V. Thermal stability of films formed by soy protein isolate-sodium dodecyl sulfate. *Polym. Degrad. Stab.* **2005**, *87*, 25–31. [CrossRef]
43. Kokoszka, S.; Debeaufort, F.; Hambleton, A.; Lenart, A.; Voilley, A. Protein and glycerol contents affect physic-chemical properties of soy protein isolate-based edible films. *Food Sci. Emerg.* **2010**, *11*, 503–510. [CrossRef]
44. Xie, D.-Y.; Song, F.; Zhang, M.; Wang, X.-L.; Wang, Y.-Z. Roles of soft segment length in structure and property of soy protein isolate/waterborne polyurethane blend films. *Ind. Eng. Chem. Res.* **2016**, *55*, 1229–1235. [CrossRef]
45. Otoni, C.G.; Avena-Bustillos, R.J.; Olsen, C.W.; Bilbao-Sáinz, C.; McHugh, T.H. Mechanical and water barrier properties of isolated soy protein composite edible films as affected by carvacrol and cinnamaldehyde micro and nanoemulsions. *Food Hydrocoll.* **2016**, *57*, 72–79. [CrossRef]